Bull. Mater. Sci., Vol. 37, No. 7, December 2014, pp. 1725–1729. © Indian Academy of Sciences.

Pr and Gd co-doped bismuth ferrite thin films with enhanced multiferroic properties

CHANG CHUN CHEN*, ZI XUAN LIU, GUI WANG and YI LIN YAN
College of Materials Science and Engineering, Nanjing University of Technology, No. 5 Xinmofan Road, Nanjing 210009, China

MS received 21 October 2013; revised 25 January 2014

Abstract. **Pr and Gd co-modified $Bi_{0.95-x}Pr_xGd_{0.05}FeO_3$ ($x = 0.00, 0.05, 0.10$) (BPGFO) thin films on Pt(111)/$Ti/SiO_2/Si(100)$ substrates were prepared by a sol-gel together with spin coating technique. A detailed study of electrical and magnetic properties of these thin films is reported. X-ray diffraction analysis shows that, with an increase in Pr content, the crystal structures of BPGFO thin films retain rhombohedral (R3c) symmetry accompanied by structure distortion. Polarization-electric field hysteresis loops of these thin films demonstrate that the incorporation of Pr and Gd into the Bi site of $BiFeO_3$ thin film could enhance the ferroelectric performance. Compared to other thin films, the optimal ferroelectric behaviours in $Bi_{0.85}Pr_{0.1}Gd_{0.05}FeO_3$ thin film are ascribed to its large dielectric constant, low dissipation factor and low leakage current density. Room temperature magnetization-magnetic field curves of these thin films indicate that all the samples are of paramagnetic behaviours and the enhanced saturation magnetic properties can be found.**

Keywords. **Pr and Gd co-modified $BiFeO_3$ thin film; ferroelectric properties; sol-gel.**

1. Introduction

In recent years, great attention has been paid to single-phase $BiFeO_3$ (BFO) multiferroic materials crystallized in the ABO_3-type perovskite structure with the R3c space group at room temperature, which display the co-existence of spontaneous electric and magnetic ordering in the same phase (Hill 2000; Fiebig *et al* 2002). The characteristics of BFO multiferroic materials with attractive functionalities caused by the interaction between electric polarization and magnetization promise some potential applications in advanced magnetoelectric devices (Eerenstein *et al* 2006). However, as promising as BFO multiferroic materials are, some drawbacks need to be overcome prior to real commercial applications. One problem is that the high leakage current in BFO materials, mainly originating from various impurity phases ($Bi_2Fe_4O_9$, $Bi_{36}Fe_{24}O_{57}$ and $Bi_{25}FeO_{40}$) as well as oxygen vacancies, results in poor ferroelectric behaviour and reliability of magnetoelectric devices (Munoz *et al* 1985; Qi *et al* 2005; Kumar and Yadav 2006). The other question is that, even though BFO is a G-type-antiferromagnetic (AFM) ordering, a weak FM component is observed owing to canting of Fe^{3+} spins at room temperature (Smolenskii and Chupis 1982; Hur *et al* 2004). As a result, it is necessary to further improve both ferroelectric and magnetic properties of BFO materials for the researchers. At present, it is well-established that an appropriate doping in BFO materials via partial ionic substitution to $Bi_{1-x}A_xFeO_3$ (A is a lanthanide ion, rare earth metal) or to $BiFe_{1-x}M_xO_3$ (M is another 3d transition metal) is a promising way for upgrading multiferroics properties (Lee *et al* 2006; Takeshi Kawae *et al* 2008).

Due to the isovalence of Gd^{3+} ions with respect to Bi^{3+} ions together with adjacent ionic radius (Gd^{3+}:1·11 Å, Bi^{3+}:1·17 Å), Gd ion doping is not expected to suppress the oxygen vacancies in BFO materials. However, the suppression of oxygen vacancies is only a cause for the decrease of the leakage current in BFO materials, the aforementioned impurity phases are also responsible for the reduction of leakage of current in BFO materials (Palkar *et al* 2004; Zhang *et al* 2006). Gd ion doping is likely to suppress the impurity phases that normally appear in BFO materials and thus reduce the leakage of current that normally happens due to the suppression of the mobile defects (such as ions of Fe^{2+}, vacancy of O and Bi) (Yuan *et al* 2006). In addition, it is also checked that the enhanced magnetization resulted from the suppression of spatially modulated spin structure that could be observed in Gd doped BFO materials (Naik and Mahendiran 2009). On the other hand, it is known that partial substitutions of Pr^{3+} at *A* site for Bi^{3+} ions of BFO materials is also an effective way to enhance the multiferroic properties of BFO materials (Yu *et al* 2008; Singh *et al* 2013). There are two reasons why enhanced multiferroic properties of BFO materials were observed: (a) the substitution of Pr^{3+} for Bi^{3+} ions will prevent the creation of defects, i.e. volatilization of Bi atoms owing to the strength of Pr–O bond (753 ± 17 kJ/mol) being higher than that of

*Author for correspondence (changchunchen@hotmail.com)

Bi–O bond (343 ± 17 kJ/mol) (Dean 1999) and (b) Pr ion doping will increase the degree of the distortion (1·126 Å for Pr^{3+} in eight coordination, 1·17 Å for Bi^{3+}) (Yu *et al* 2008), resulting in a smaller bond angle of Fe–O–Fe and a significant magnetization As a result, it is fascinating to study the effect of co-substitution of Pr and Gd on BFO materials in order to have the combined advantages of Gd and Pr ion dopants. In this paper, we report preparations of Pr and Gd co-doped $Bi_{0·95-x}Pr_xGd_{0·05}FeO_3$ ($x = 0·00$, 0·05, 0·10) thin films on Pt(111)/Ti/SiO_2/Si(100) substrates and their enhanced ferroelectric and magnetic properties.

2. Experimental

Pr and Gd co-modified $Bi_{0.95-x}Pr_xGd_{0·05}FeO_3$ ($x = 0·00$, 0·05, 0·10) (BPGFO) thin films on Pt(111)/Ti/SiO_2/Si(100) substrates were prepared by a sol-gel together with spin coating technique. Bismuth nitrate [$Bi(NO_3)_3·5H_2O$] (Aldrich, 99·99%), ferric nitrate [$Fe(NO_3)_3·9H_2O$] were used as the raw materials. $Gd(NO_3)_3·6H_2O$ and $Pr(NO_3)_3$ were used as the dopants. 2-methoxyethanol ($C_3H_8O_2$) and acetic anhydride [$(CH_3CO)_2O$] were employed as the solvent and dehydrating agent, respectively. During the preparation of precursor solutions of Pr and Gd co-modified BPGFO thin films, a fixed amount of bismuth nitrate and ferric nitrate were firstly dissolved in 2-methoxyethanol ($C_3H_8O_2$) under constant stirring until fully dissolved, and then joined an appropriate $Gd(NO_3)_3·6H_2O$ and $Pr(NO_3)_3$ into the completely dissolved solutions with fixed molar ratios of metal ions [$n(Bi^{3+}): n(Pr^{3+}): n(Fe^{3+}): n(Gd^{3+}) = 0·95-x: x: 1: 0·05$ ($x = 0·00, 0·05, 0·10$)]. It is worth noting that an excess of 5 wt% Bi was added to these solutions to compensate for some unavoidable bismuth oxide loss during the follow-up thermal treatment. Subsequently, a nominal amount of acetic anhydride [$(CH_3CO)_2O$] was joined into the above-mentioned solutions for dehydrating and appropriate quantity of 2-methoxyethanol was replenished into the formed hybrid solutions to adjust the Fe^{3+} ions concentration to expected 0·3 mol/L. Subjected to full stirring and 24 h aging, the Pr and Gd co-modified $Bi_{0·95-x}Pr_xGd_{0·05}FeO_3$ ($x = 0·00$, 0·05, 0·10) precursor solutions were successfully made.

Prior to preparing the BPGFO thin films, the Pt(111)/Ti/SiO_2/Si(100) substrates were cleaned by ultra-sonication in acetone and alcohol and dried with nitrogen gas. And then, the BPGFO precursor solutions were spin-coated on the cleaned Pt(111)/Ti/SiO_2/Si(100) substrates at a rate of 3300 rpm for 15 s. The wet films were preheated over a hotplate at 350 °C for 5 min, followed by a pyrolysis process at 500 °C for 5 min. The coating and thermal treatment process was repeated twelve times and then these films were annealed at 600 °C for 20 min in air by a rapid thermal annealing process for full crystallization. Finally, the thickness of resultant films was around 230 nm.

The crystal structures of Pr and Gd co-modified BPGFO thin films were investigated by the $\theta-2\theta$ method of XRD with a CuKα_1 ($\lambda = 0·15406$ nm) source at 40 kV and 30 mA using a multi-purpose XRD system (D/MAX-RB). For electrical measurements, a gold thin film was coated on the surface of these samples with an area of $5·25 \times 10^{-5}$ cm^{-2} using a shadow mask and then sintered at 550 °C for 15 min in an N_2 atmosphere. The ferroelectric hysteresis loops together with leakage current behaviours of these thin films were obtained using a ferroelectric tester (Radiant Technologies, RT66A). The dielectric constant and the dissipation factor were measured using an HP4294A impedance analyzer. A vibrating sample magnetometer (VSM) was employed to measure the magnetic properties. All the measurements were performed at room temperature.

3. Results and discussion

Figure 1 shows the XRD patterns of Pr and Gd co-modified $Bi_{0·95-x}Pr_xGd_{0·05}FeO_3$ ($x = 0·00$, 0·05, 0·10) (BPGFO) thin films grown on Pt(111)/Ti/SiO_2/Si(100) substrates. All the diffraction peaks are identified and indexed according to the standard diffraction pattern data (Sosnowska *et al* 1996). The XRD patterns indicate that these BPGFO thin films are polycrystalline with a perovskite structure belonging to the space group of R3c. The diffraction peaks from well-documented impurity phases such as $Bi_2Fe_4O_9$ (Fe-rich phase) and $Bi_{36}Fe_{24}O_{57}$ (Bi-rich phase) were not detected. When magnifying the (110) diffraction peaks around $2\theta = 32°$ (figure 1), it was observed that the (110) peak shifted towards high diffraction angles gradually with increasing Pr concentration. This phenomenon indicates that Pr doping leads to some kind of structural distortion. The diffraction peak shifting towards high diffraction angles is due to the decrease of BPGFO lattice spacing. Both the ionic radius of Gd^{3+} (1·11 Å) and that of Pr^{3+} (1·126 Å) are smaller than that of Bi^{3+} (1·17 Å) (Yu *et al* 2008). And thus, the decrease of BPGFO lattice spacing may be attributed to the incorporation of Pr and Gd ions into the A-site of BFO

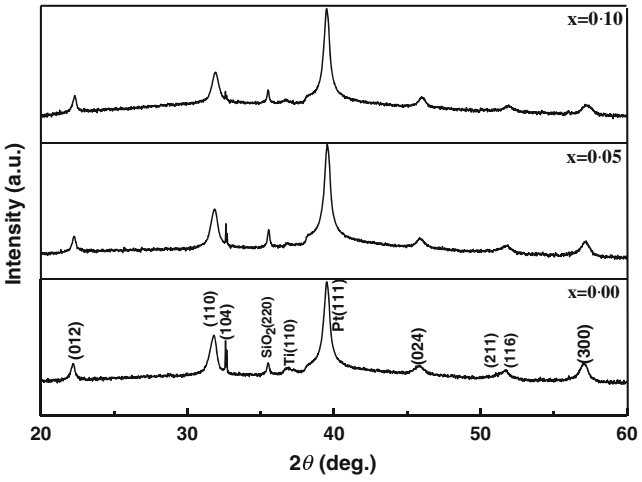

Figure 1. X-ray diffraction patterns of the $Bi_{0·95-x}Pr_xGd_{0·05}FeO_3$ ($x = 0·00$, 0·05, 0·10) thin films grown on Pt(111)/Ti/SiO_2/Si(100) substrates.

materials. In addition, with an increase of Pr doping concentration in $Bi_{0.95-x}Pr_xGd_{0.05}FeO_3$, the intensity of (104) diffraction peaks were found to gradually decrease.

Figure 2 shows the ferroelectric behaviour of Pr and Gd co-modified BPGFO thin films as a function of electric field. For the Gd co-modified $Bi_{0.95}Gd_{0.05}FeO_3$ ($x = 0{\cdot}00$) thin films, a ferroelectric hysteresis loop is observed with saturation polarization of $5{\cdot}8\,\mu C/cm^2$. With an increased concentration of Pr in Pr and Gd co-modified $Bi_{0.95-x}Pr_xGd_{0.05}FeO_3$ ($x = 0{\cdot}05$), the saturation polarization value increases to $6{\cdot}03\,\mu C/cm^2$. When the substitution of a Bi site by Pr ion with a concentration of 0·10, the saturation polarization value in the Pr and Gd co-modified $Bi_{0.95-x}Pr_xGd_{0.05}FeO_3$ thin film increases to $7{\cdot}36\,\mu C/cm^2$. Consequently, the incorporation of Pr ions into the Bi site of the BFO thin film is noticeably attributed to the improvement of ferroelectric performance of pure BFO thin films. Compared to the saturation polarization value of $Bi_{0.95}Gd_{0.05}FeO_3$ thin film, the enhanced saturation polarization values in $Bi_{0.90}Pr_{0.05}Gd_{0.05}FeO_3$, $Bi_{0.85}Pr_{0.1}Gd_{0.05}FeO_3$ thin films are probably ascribed to their low leakage current density (figure 4).

Figure 3 shows the variation of dielectric constant (ε_r) and dissipation factor ($\tan\delta$) as a function of applied frequency for the Pr and Gd co-modified BPGFO thin films measured at room temperature. In the low frequency range, both ε_r and $\tan\delta$ have very high values. With an increase of applied frequency, ε_r together with $\tan\delta$ for all the thin films gradually decrease and then they are nearly constant at high frequencies. This decrease in the dielectric constant in the frequency range is likely caused by space charge polarization or Maxwell Wagner type interfacial polarization (Okatan *et al* 2010). The decrease in $\tan\delta$ correlates with the corresponding changes in the electrical resistivity. At a fixed frequency, ε_r of $Bi_{0.85}Pr_{0.1}Gd_{0.05}FeO_3$ thin films is the largest, which is beneficial to its optimal saturation polarization values (online 2Pr), shown in figure 2. On the other hand, at a fixed frequency, $\tan\delta$ of the $Bi_{0.85}Pr_{0.1}Gd_{0.05}FeO_3$ thin films is also the least. Consequently, the largest dielectric constant value of the $Bi_{0.85}Pr_{0.1}Gd_{0.05}FeO_3$ thin films coincides with its least dissipation factor. Higher dissipation factors generally represent large leakage current due to higher conductivity. A decrease in the value of dissipation factor for Pr and Gd co-modified BPGFO thin films suggests that Pr substitution is helpful in reducing the leakage current. Consequently, the ferroelectric material with the largest dielectric constant together with the least dissipation factors is advantageous for any device application.

Figure 4 shows the *I–V* characteristics of Au/Pr and Gd co-modified BPGFO thin films/Pt capacitors annealed at 550 °C for 15 min in an N_2 atmosphere and measured at room temperature. The leakage current density of all the capacitors increases rapidly with an increase in the initially applied electric field. The leakage current densities of $Au/Bi_{0.95}Gd_{0.05}FeO_3/Pt$, $Au/Bi_{0.9}Pr_{0.05}Gd_{0.05}FeO_3/Pt$, $Au/Bi_{0.85}Pr_{0.10}Gd_{0.05}FeO_3/Pt$, capacitor at the maximum applied field 350 kV/cm are about $9{\cdot}38 \times 10^{-5}$, $1{\cdot}75 \times 10^{-6}$, $5{\cdot}97 \times 10^{-7}$ A/cm^2, respectively. It is well known that a mixed-valence state of $Fe^{2+/3+}$ exists in the pure BFO materials due to the presence of oxygen and Bi vacancies. Electron transfer probably takes place between these ions and thus pure BFO presents higher conductivity. Gd^{3+} ions and Pr^{3+} co-substitution at Bi-site lead to the suppression in Bi-volatilization and the oxygen vacancies. As a result, the Pr and Gd co-modified BPGFO thin film exhibits a lower leakage current density. The lower leakage current density brings about lower dielectric loss values in Pr and Gd co-modified BPGFO thin films as shown in figure 3. The lower dielectric loss at a low frequency of

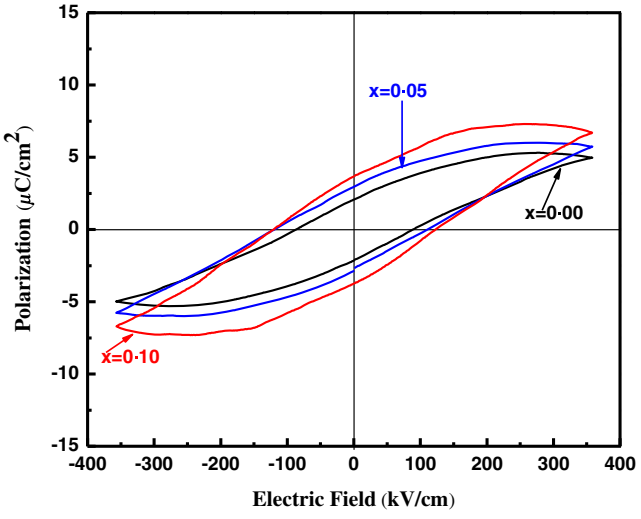

Figure 2. Electric hysteresis loops of $Bi_{0.95-x}Pr_xGd_{0.05}FeO_3$ ($x =$ 0·00, 0·05, 0·10) thin films grown on Pt(111)/Ti/SiO_2/Si(100) substrates.

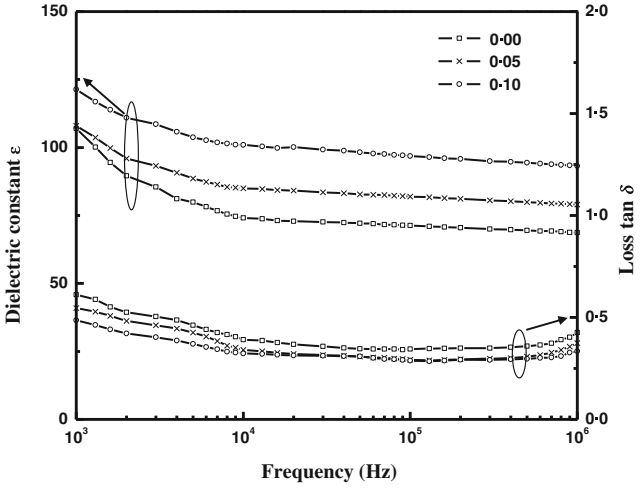

Figure 3. Dielectric constant (ε_r) and dissipation factor ($\tan\delta$) in dependence of frequency for the $Bi_{0.95-x}Pr_xGd_{0.05}FeO_3$ ($x = 0{\cdot}00, 0{\cdot}05, 0{\cdot}10$) thin films grown on Pt(111)/Ti/SiO_2/Si(100) substrates.

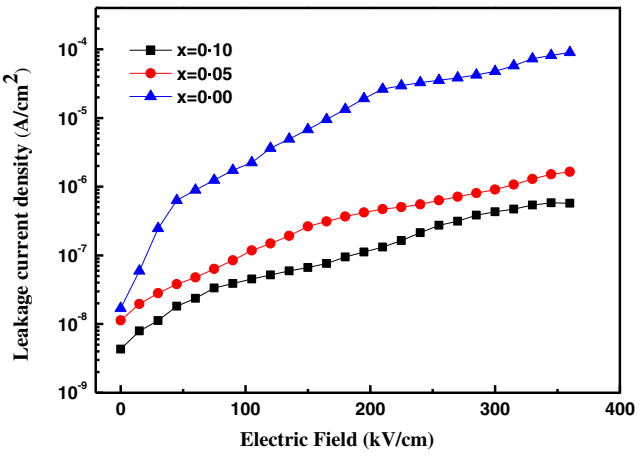

Figure 4. *I–V* characteristics of the $Bi_{0.95-x}Pr_xGd_{0.05}FeO_3$ ($x=$ 0·00, 0·05, 0·10) thin films grown on Pt(111)/Ti/SiO_2/Si(100) substrates.

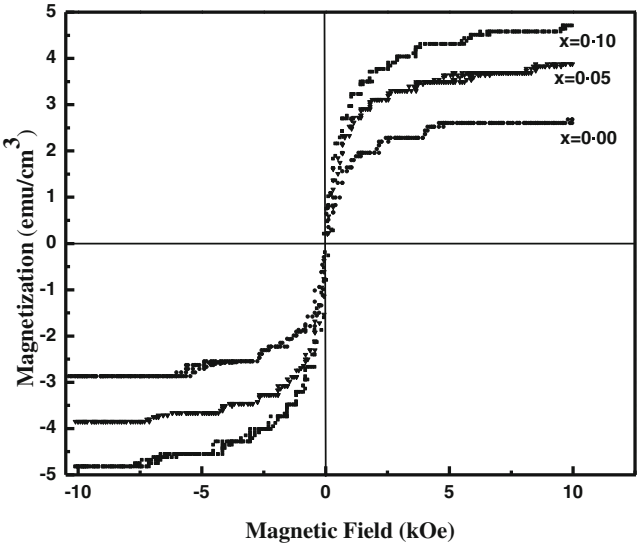

Figure 5. Magnetization variation with applied magnetic field of the $Bi_{0.95-x}Pr_xGd_{0.05}FeO_3$ ($x=$ 0, 0·05, 0·10) thin films on Pt(111)/Ti/SiO_2/Si(100) substrates at room temperature.

$BiFeO_3$ thin films at room temperature reflects their lower leakage currents (Yun *et al* 2004).

Room temperature magnetization–magnetic field (*M–H*) curves of Pr and Gd co-modified BPGFO thin films measured with magnetic field of 10 kOe are shown in figure 5. Owing to the remanant magnetization (M_r) and coercive field (H_c) nearly being equal to zero, all the BPGFO thin film samples show weak hysteresis loops representing paramagnetic behaviour. With an increase of Pr doping content in $Bi_{0.95-x}Pr_xGd_{0.05}FeO_3$ thin film, an enhanced saturation magnetization is observed in figure 5. It is well-established that the spin cycloid of BFO, with latent magnetization locked within the cycloid, is related to its R3c structure, substituents can perturbate its spiral spin structure and, if it is destructed, the magnetization tends to increase (Wang *et al* 2005). In our study, because of the incorporation of Pr and Gd ions into the A-site of BFO materials and with an increase of Pr doping concentration in $Bi_{0.95-x}Pr_xGd_{0.05}FeO_3$ ($x=0{\cdot}00, 0{\cdot}05, 0{\cdot}10$) thin films, the structural distortion originated from decreases in lattice spacing. Consequently, it is reasonable that the improved magnetic properties BPGFO thin films could be obtained in figure 5. For the merit of co-doping in BFO thin film, the enhanced saturation magnetization values are also found in the other Co–Pr substituted thin films (Neeraj Panwar *et al* 2012).

4. Conclusions

In summary, the Pr and Gd co-modified $Bi_{0.95-x}Pr_xGd_{0.05}FeO_3$ ($x=0{\cdot}00$, 0·05, 0·10) thin films grown on Pt(111)/Ti/SiO_2/Si(100) substrates were synthesized by a sol-gel together with a spin-coating method and their structures and properties were studied. When varying the substitution of a Bi site by Pr ions in $Bi_{0.95-x}Pr_xGd_{0.05}FeO_3$ ($x=0{\cdot}00, 0{\cdot}05, 0{\cdot}10$) thin films, the structural distortion and an enhanced ferroelectric polarization at room temperature could be found. In addition, with an increase in Pr content, the dielectric constant increases, whereas both leakage current density and the dielectric loss decrease. The enhanced saturation magnetic properties are also observed for the Pr and Gd co-modified $Bi_{0.95-x}Pr_xGd_{0.05}FeO_3$ ($x=$ 0·00, 0·05, 0·10) thin films with an increase in Pr content.

Acknowledgements

This study is partially financed by the Priority Academic Program Development of Jiangsu Higher Education Institutions (PAPD), China, and also partially supported by University Students' innovative undertaking training program of higher education of Jiangsu Province (granted number: 201410291004Z).

References

Dean J A 1999 *Lange's handbook of chemistry* 15th edn (New York: McGraw-Hill)

Eerenstein W, Mathur N D and Scott J F 2006 *Nature* **442** 759

Fiebig M, Lottermoser Th, Fröhlich D, Goltsev A V and Pisarev R V 2002 *Nature* **419** 818

Hill N A 2000 *J. Phys. Chem.* **B104** 6694

Hur N, Park S, Sharma P A, Ahn J S, Guha S and Cheong S W 2004 *Nature* **429** 392

Kumar M and Yadav K L 2006 *J. Appl. Phys.* **100** 074111

Lee Y-H, Wu J-M and Lai C-H 2006 *Appl. Phys. Lett.* **88** 042903

Munoz T, Rivera J P, Monnier A and Schmid H 1985 *Jpn. J. Appl. Phys. Part 1* **24** 1051

Naik V B and Mahendiran R 2009 *Solid State Commun.* **149** 754

Neeraj Panwar, Indrani Coondoo, Amit Tomar, Kholkin A L, Venkata S Puli and Ram S Katiyar 2012 *Mater. Res. Bull.* **47** 4240

Okatan M B, Mantese J V and Alpay S P 2010 *Acta Materialia* **58** 39

Palkar Y R, Kundaliya D C, Malik S K and Bhattacharya S 2004 *Phys. Rev.* **B69** 212102

Qi X D, Dho J, Tomov R, Blamire M G and MacManus-Driscoll J L 2005 *Appl. Phys. Lett.* **86** 062903

Singh V, Sharma S, Kumar M, Dwivedi R K and Kotnala R K 2013 *Phys. Status Solidi.* **A210** 1442

Smolenskii G A and Chupis L 1982 *Soviet Physics Uspekhi* **25** 475

Sosnowska I, Przenioslo R, Fischer P and Murashov V A 1996 *J. Magn. Magn. Mater.* **160** 384

Takeshi Kawae, Hisashi Tsuda, Hiroshi Naganuma, Satoru Yamada, Minoru Kumeda, Soichiro Okamura and Akiharu Morimoto 2008 *Jpn. J. Appl. Phys.* **47** 7586

Wang N, Cheng J, Pyatakov A, Zvezdin A K, Li J F, Cross L E and Viehland D 2005 *Phys. Rev.* **B72** 1044341

Yu B, Li M, Hu Z, Pei L, Guo D, Zhao X and Dong S 2008 *Appl. Phys. Lett.* **93** 182909

Yuan G L, Or S W, Wang Y P, Liu Z G and Liu J M 2006 *Solid State Commun.* **138** 76

Yun K Y, Noda M, Okuyama M, Saeki H, Tabata H and Saito K 2004 *J. Appl. Phys.* **96** 3399

Zhang S-T, Zhang Y, Liu M, Du C, Chen Y, Liu Z, Zhu Y and Ming N-B 2006 *Appl. Phys. Lett.* **88** 162901